International Symposium COMODIA 90: 499-504(1990)

An Assessment of Discretisation Schemes and Turbulence Models for In-Cylinder Flows

A.P.Watkins, P.Kanellakopoulos and C.J.Lea

Mechanical Engineering Department
University of Manchester
Institute of Science and Technology
Manchester M60 1QD
U.K.

ABSTRACT

The errors inherent in the calculation of flows inside the cylinders of reciprocating i.c. engines are assessed in this paper. For this purpose is calculated a simple steady flow past a valve into an open-ended cylinder.

It is concluded that many of the current procedures based on relatively coarse grids, eddy-viscosity turbulence models and diffusive first order spatial discretization schemes cannot hope to accurately capture the intake flow. Rather, accuracy can only be obtained if the quadratic QUICK spatial discretization scheme is used for the mean flow velocity components, and a differential stress model of turbulence is employed. Even then relatively fine grids, compared with current practice, are required.

INTRODUCTION

Over recent years a number of computer codes have been developed which solve three-dimensional equations for the fluid flow in internal combustion engine cylinders. Some of these codes are used regularly by engine manufacturers as aids to design of engine geometry.

Presumably, because of the complexity of the time-varying flow being calculated, most of these codes employ fairly crude models for many aspects of the flow calculations. For example, highly stable, but numerically inaccurate first order spatial discretization schemes are almost universally employed. At best turbulence models based on eddy-viscosity-type approaches are used. These are known to be inaccurate for the calculation of complex recirculating flows. At worst, 'turbulence' is calculated by some false viscosity method. Given the important role of the turbulence in enhancing combustion and heat transfer rates, it is extremely doubtful whether such approaches are really capable of giving the required detailed information.

Such three-dimensional calculation procedures may well be capable of predicting the gross mean flow characteristics, and even of predicting mean flow trends with design change, however it is often the secondary flow motions which are important, along with the turbulence fields.

One should be aware therefore of the potential sources of errors which these codes may embody.

Truncation errors are caused when either the computational grid is too coarse, or it is badly positioned. In the latter category might be grids which do not match boundaries, i.e. are not boundary fitted, or are poorly distributed, thus failing to capture important phenomena. Additional truncation errors arise from using too large steps in time. Further errors may be caused if the flow equations do not match the physics of the flow. Particular attention is required here to the modelling of the turbulence of the flow. Numerical diffusion may arise because of the way approximations are made when the partial differential equations are converted to finite algebraic equations. Finally the imposition of incorrect boundary conditions on the flow causes yet further errors. Some attempts have been made to reduce inlet boundary condition errors by calculating flow in the inlet port as well as the cylinder. However this increases the size of the computer storage and computation times, and often a compromise is made which results in fewer grid nodes being employed in the cylinder, thus increasing truncation errors there. Other codes continue to use measured or assessed velocity component profiles at the valve curtain, as the inlet boundary condition.

In this paper a number of these error sources are considered and their effects on calculated flow results are assessed. For this exercise a fairly simple geometry has been chosen, namely axisymmetric steady flow past a single valve into an open-ended cylinder. Intake flow is a crucial aspect of flow management in spark-ignition engines, contributing much to the nature of the turbulent flow near TDC, where combustion takes place. The unsteadiness of real i.c. engine intake flows does of course influence the end result, as does the three-dimensional nature of the flow. However the main features of unsteady 3D enclosed intake flow are reproduced by steady 2D open-ended flow, and the latter has the great advantage of simplicity. It allows much finer grids to be used, for example, without consuming prohibitive amounts of computing time. In addition the experimental data is generally more extensive and accurate, thus allowing for a more detailed assessment of the error sources.

Calculated results are compared with experimental data obtained from a model engine by means of LDA at Imperial College (1).

MATHEMATICAL MODEL

Turbulence Models

The governing equations for the incompressible, steady state, turbulent flow studied in this paper are the time-averaged continuity and Navier-Stokes momentum equations, in Cartesian tensor form;

$$\frac{\partial \bar{U}_i}{\partial x_i} = 0.0 \qquad (1)$$

$$\frac{\partial \bar{U}_i \bar{U}_j}{\partial x_j} = -\frac{\partial \bar{P}}{\partial x_i} + \frac{\partial}{\partial x_j}\left[\nu \frac{\partial \bar{U}_i}{\partial x_j} - \overline{u_i u_j}\right] \qquad (2)$$

The turbulent correlations $\overline{u_i u_j}$, in the form $\rho\ \overline{u_i u_j}$ known as the Reynolds stresses, which appear in equation (2) are unknown and so to provide a closed set of equations, modelled forms for $\overline{u_i u_j}$ are required. The turbulence models which have been used to effect closure of the equation set are fundamentally quite different and are presented below.

The k-ϵ model (2) is based on the eddy viscosity concept;

$$\nu_t = C_\mu \frac{k^2}{\epsilon} \tag{3}$$

where k and ϵ are determined from the solution of the semi-empirical transport equations;

$$\frac{\partial U_j k}{\partial x_j} = \frac{\partial}{\partial x_j}\left(\frac{\nu_t}{\sigma_k}\frac{\partial k}{\partial x_j}\right) + \left[\nu_t\left(\frac{\partial U_i}{\partial x_j} + \frac{\partial U_j}{\partial x_i}\right) - \frac{2}{3}\delta_{ij}k\right]\frac{\partial U_i}{\partial x_j} - \epsilon \tag{4}$$

$$\frac{\partial U_j \epsilon}{\partial x_j} = \frac{\partial}{\partial x_j}\left(\frac{\nu_t}{\sigma_\epsilon}\frac{\partial \epsilon}{\partial x_j}\right) + C_{\epsilon 1}\frac{\epsilon}{k}\left[\nu_t\left(\frac{\partial U_i}{\partial x_j} + \frac{\partial U_j}{\partial x_i}\right) - \frac{2}{3}\delta_{ij}k\right]\frac{\partial U_i}{\partial x_j} - C_{\epsilon 2}\frac{\epsilon^2}{k} \tag{5}$$

with constants $C_{\epsilon 1}$=1.44, $C_{\epsilon 2}$=1.92, C_μ=0.09, σ_k=1.0, σ_ϵ=1.22.

The Reynolds stresses are then found by application of the Boussinesq hypothesis;

$$-\overline{u_i u_j} = \nu_t\left(\frac{\partial U_i}{\partial x_j} + \frac{\partial U_j}{\partial x_i}\right) - \frac{2}{3}\delta_{ij}k \tag{6}$$

The Algebraic Stress Model (ASM) proposed by Rodi (3) and the Differential Stress Model (DSM) (4) both seek to model the exact transport equations for the Reynolds stresses. The form of the DSM employed here is shown by considering the following exact transport equation for $\overline{u_i u_j}$,

$$C_{ij} + D_{ij} = P_{ij} + \Phi_{ij} + \epsilon_{ij} \tag{7}$$

and its modelled form;

$C_{ij} = \frac{\partial}{\partial x_k}(U_k\ \overline{u_i u_j}) \Rightarrow$ treated exactly, no modelling needed.

$P_{ij} = -\left(\overline{u_j u_k}\frac{\partial U_i}{\partial x_k} + \overline{u_i u_k}\frac{\partial U_j}{\partial x_k}\right) \Rightarrow$ treated exactly, no modelling req.

$D_{ij} = -C_s\frac{\partial}{\partial x_k}\left(\frac{k}{\epsilon}\overline{u_k u_\ell}\frac{\partial \overline{u_i u_j}}{\partial x_\ell}\right) \Rightarrow$ Modelled, Daly & Harlow (5)

$\Phi_{ij} = \Phi_{ij_1} = -C_1\frac{\epsilon}{k}\left(\overline{u_i u_j} - \frac{2}{3}\delta_{ij}k\right) \Rightarrow$ Modelled, Rotta (6)

$+\ \Phi_{ij_2} = -C_2\left(P_{ij} - \frac{1}{3}\delta_{ij}P_{kk}\right) \Rightarrow$ Modelled Naot et al (7)

$\epsilon_{ij} = -\frac{2}{3}\delta_{ij}\epsilon \Rightarrow$ Modelled, Launder et al (8)

along with the modelled ϵ equation (8);

$$\frac{\partial U_k \epsilon}{\partial x_k} = C_\epsilon\frac{\partial}{\partial x_k}\left(\frac{k}{\epsilon}\overline{u_k u_\ell}\frac{\partial \epsilon}{\partial x_\ell}\right) + C_{\epsilon 1}\frac{\epsilon}{k}\left(-\overline{u_i u_k}\frac{\partial U_i}{\partial x_k}\right) - C_{\epsilon 2}\frac{\epsilon^2}{k} \tag{8}$$

DSM constants are C_1=1.8, C_2=0.6, C_S=0.22, $C_{\epsilon 1}$=1.45, $C_{\epsilon 2}$=1.9, C_ϵ=0.15.

The ASM relates stress transport algebraically to that of k;

$$C_{ij} = \frac{\overline{u_i u_j}}{k} C_k \qquad D_{ij} = \frac{\overline{u_i u_j}}{k} D_k \tag{9}$$

where C_k and D_k are respectively the convective and diffusive transport of k.

This allows one to rearrange the modelled transport equations for $\overline{u_i u_j}$ into sets of algebraic relationships. This means that the only turbulent transport equations to be solved are those for k and ϵ.

Of the three models described, the DSM has the most comprehensive applicability (4), the ASM suffering from the stress transport assumption (9), and the k-ϵ model from the more limiting eddy viscosity hypothesis. However the DSM level of closure has the disadvantage that three more coupled transport equations have to be solved.

Numerical Models

The flow equations are solved by the finite volume technique which reduces the partial differential equations to algebraic equations which are then solved by employing the Tri-Diagonal Matrix Algorithm in an alternating direction fashion.

The discretization method for the convection terms is of particular importance, especially for the momentum equations. Three techniques have been used; the Power Law Difference Scheme (PLDS) of Patankar (10) and the Quadratic Interpolation Scheme (QUICK) of Leonard (11) for the k-ϵ and ASM calculations, and in the DSM calculations, the HYBRID method of Patankar and Spalding (12). The PLDS and HYBRID schemes are similar and employ the 2nd order accurate central difference scheme at low cell Peclet number and the 1st order upwind scheme with zero diffusion at high Peclet number. The essential difference between PLDS and HYBRID is the change-over point between central differencing and upwinding; for uniform grids this occurs at cell Peclet number of 10 for PLDS and 2 for HYBRID. The QUICK scheme is based on the use of an upstream shifted parabolic interpolation for each control volume face, is third order accurate, and hence free from the numerical diffusion which affects PLDS and HYBRID in the upwind part of these schemes. However QUICK is an unbounded scheme and leads to numerical stability problems, especially for the DSM calculation, hence the HYBRID scheme has been used for results presented with this turbulence model. Also, where QUICK is used with the k-ϵ and ASM computations, it is employed only in the momentum equations, the turbulence equations are source term dominated and using PLDS should introduce little error.

Inlet boundary conditions have been supplied by the experimental results (1). These consisted of both momentum components and axial and radial turbulence intensities measured at a radial plane 0.5mm above the valve inlet plane.

The codes employed here use a staggered grid arrangement to enhance stability (10), so that for the majority of the computations the experimental boundary conditions for the axial velocity component and the turbulence intensities are employed at a radial plane 0.55mm below the valve inlet plane. The radial velocity component is imposed at the valve inlet plane (See Fig. 1). Some of the DSM results use the experimental inlet conditions in a more exact manner, that is, at the experimental measurement plane.

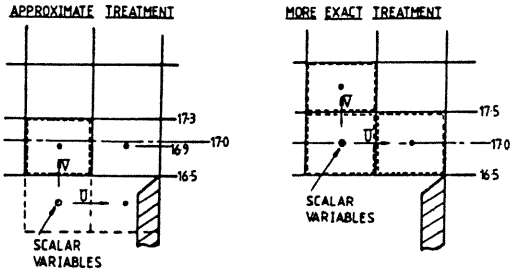

Fig. 1: Alternative positions of inlet boundary conditions

The other boundaries are treated in a standard fashion, however a 2-layer wall function is employed to bridge the gap between the main flow and solid walls in the DSM calculations.

The criterion for convergence for both codes is that the separate sums of the normalised residual sources for the momentum components and mass flux are less than $1x10^{-3}$, normalisation being by the incoming flux. The turbulent shear stress control volume in the case of the ASM and DSM, is staggered relative to both the velocity components and the scalar unknowns. Turbulent normal stresses are evaluated at the scalar nodes and to further stabilise the DSM calculation these stress component source terms are tested for positive and negative contributions and separated into the appropriate parts of the linearised source term.

RESULTS AND DISCUSSION

Discretization

Comparison of discretization models was carried out on an axisymmetric 63x41 line grid as shown in Fig. 2. The k-ϵ turbulence model was employed. Experimentally-measured radial profiles are available (1) of axial and radial mean flow and turbulence intensities at 6mm and 15mm from the cylinder head. The former coincides with the valve face.

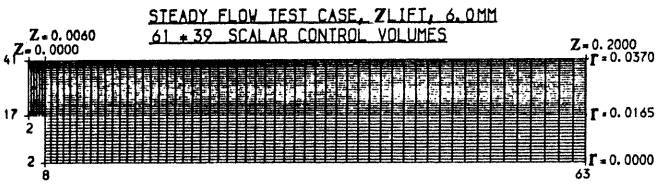

Fig. 2: Grid arrangement

Figure 3 illustrates the performance of the three discretization models used. Here axial mean flow velocities and turbulence intensities profiles at 15mm are shown. For the mean flow, use of the QUICK scheme reduces the calculated spread of the intake jet from that produced by either of the other schemes. This is undoubtedly due to the removal of numerical diffusion. It is probable that some of the remaining discrepancy with experiment is due to grid space truncation errors. As will be shown later, much of the underprediction of the peak velocity is also due to this source.

As for the turbulence intensity profiles, it is evident that none of the schemes is capable of adequate prediction, when combined with the k-ϵ turbulence model. The QUICK scheme again produces the better results, in terms of both quantity and quality, capturing at least some of the two peaks.

The dominant feature of the flow at this measurement location is the oblique impingement of the inlet jet on the cylinder wall. This creates a complex structure of shear and normal stresses on the flow, leading to high levels of turbulence generation. Much of this generation is due to normal stresses. The k-ϵ model in its standard form cannot

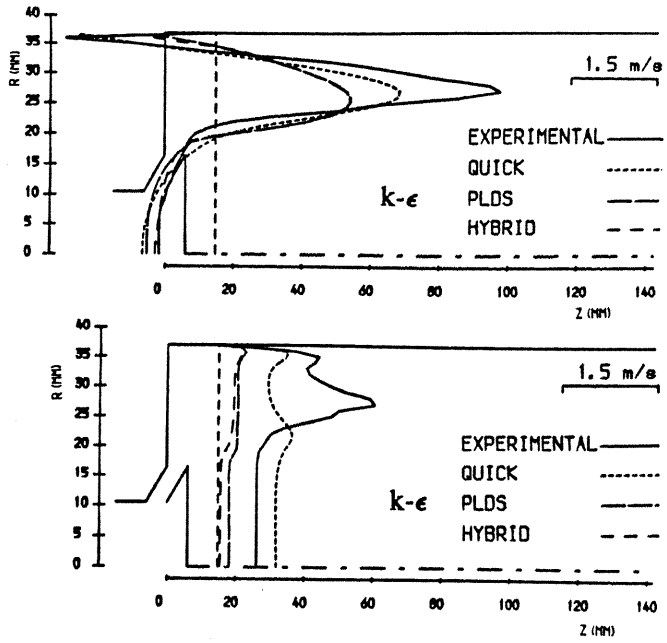

Fig. 3: Comparison of discretization schemes, with k-ϵ

cope with this feature. It may be that augmentation of turbulence generation by normal stresses is required in the model, perhaps along the lines suggested by Hanjalic and Launder (13).

The agreement with experimental data here is much worse than that obtained by Gosman et al (14) and El-Tahry (15). However the valve seat angle in that model engine was 30° to the cylinder centreline. This resulted in the impingement occurring much further down the cylinder wall away from the cylinder head. At this location the jet has spread much further and is relatively weaker. The results of these features are that the turbulence intensities are about half the level found in the case examined here. The implication is that the normal stresses play a reduced role in that case.

Grid refinement. The same calculations as above were repeated on a finer grid of 101x61 lines. Grid spacings and hence the cell Peclet numbers are thus reduced by factors of 3/5 and 2/3 of the original values in the z and r directions respectively. Considerable reductions in numerical diffusion are therefore to be expected when using the HYBRID or PLDS schemes. Indeed large improvements are obtained in mean flow velocity predictions, as shown in Fig. 4. However these results are still inferior to those using the QUICK scheme, where reductions in truncation errors lead to the prediction of a thinner, faster jet.

Fig. 4 also illustrates that the grid spacings have a profound influence on the turbulence intensity predictions, using HYBRID or PLDS. Turbulence levels are much improved and evidence of both peaks is now seen. However the QUICK scheme still seems to give a marginally better prediction.

The fact that such large changes can be made in predictions by using grids finer than 63x41 lines must throw some doubt on predictions obtained by in-cylinder flow codes using much fewer lines in any given direction, if they employ HYBRID or PLDS schemes combined with eddy-viscosity turbulence models.

Turbulence Models

To assess the effects of the turbulence model employed, the same case was re-run on the coarser grid with the k-ϵ model replaced by the ASM or DSM. For the ASM runs, QUICK was used throughout, except for the turbulence model

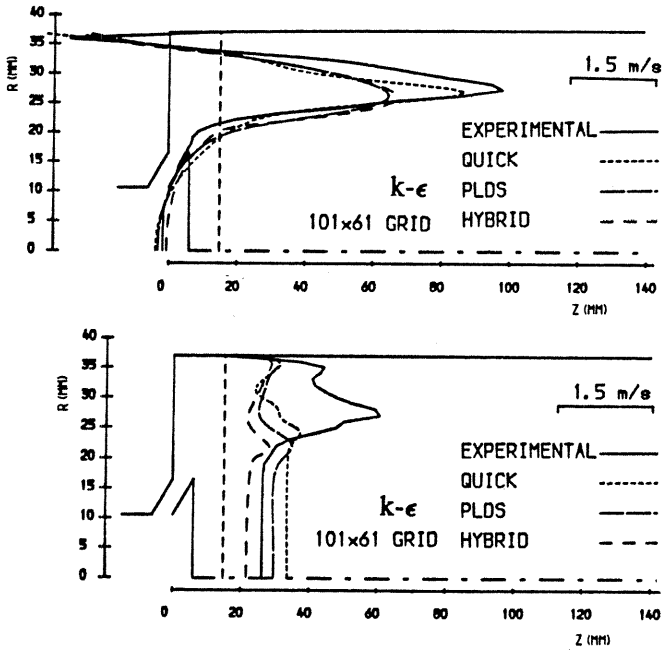

Fig. 4: Comparison as Fig. 3, but on a finer grid

equations, which employed PLDS. The DSM runs used the HYBRID scheme throughout.

It is evident from Fig. 5 that the use of ASM does not produce any major improvement over the k-ε results. Indeed the turbulence intensity predictions are markedly inferior in the near-wall region.

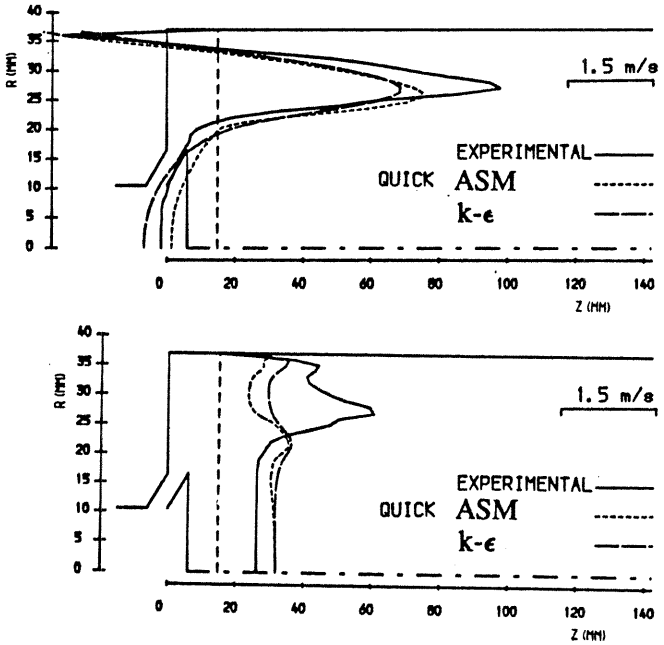

Fig. 5: Comparison of k-ε and ASM turbulence models, with QUICK

Fig. 6 shows the results of DSM calculations. To isolate the effects of the discretization scheme from those of the turbulence model, comparison is made with ASM predictions, produced using the PLDS scheme throughout. It is evident that the mean flow is less well predicted by the DSM. The vortex in the cylinder head/wall corner is predicted as being considerably shorter than either the ASM predictions or the experimental results.

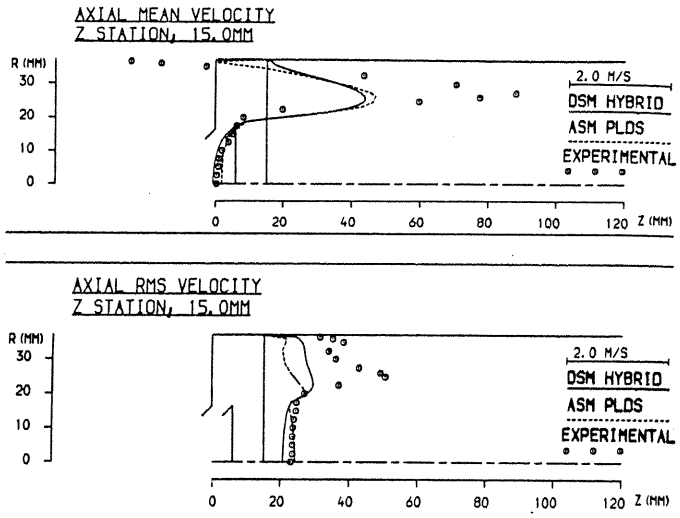

Fig. 6: Comparison of DSM and ASM turbulence models

It may be that the use of the HYBRID scheme with the DSM results in greatly increased numerical diffusion. Fig. 7 shows that central differencing is used over a minority of the flow domain, particularly for the axial cell faces. This is because in the DSM the cell Peclet number is composed with the laminar viscosity not the turbulent viscosity, as in k-ε or the ASM. Greatly improved results are therefore to be expected using QUICK with the DSM. This is a subject of current research, results of which will be reported later.

Despite the shortcomings of the mean flow predictions the turbulence intensity predictions using the DSM in Fig. 6 are nearly everywhere superior to those of the ASM. This is particularly so in the near-wall region, where the experimental values are now generally underpredicted by less than 50%.

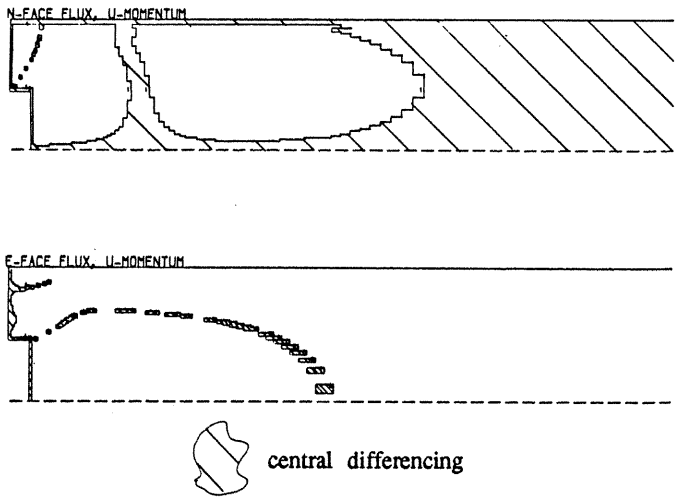

Fig. 7: Areas in which central differencing is used in Hybrid scheme with DSM

Inlet conditions. As was stated above, due to the staggered nature of the grid, not all the inlet boundary conditions have been imposed at the same plane, nor indeed at the measuring plane. To assess this feature, a further run was made using the DSM, in which all the boundary conditions are imposed at the location where they were measured, apart from that of the radial velocity component which was imposed 1.0mm from the valve curtain, due to the staggered grid arrangement. As can be seen, by comparing Fig. 8 with Fig. 6, the main effects are to increase

the mean axial momentum, and the resulting turbulence intensities. In fact, due the overly thick jet, the entrainment in the region near the valve face is over-predicted resulting in too large a backflow there. As before the backflow in the corner is too little.

On the other hand the turbulence intensities are now much better predicted, both in quantity and shape, particularly in the jet region.

The strange kink in the mean flow profile near the wall is due to a mis-match of conditions across the laminar sub-layer. If a larger spacing is imposed next to the wall so that the values of non-dimensional distance y^+ lie in the turbulent region then the kink is virtually eliminated, without any perceptible differences being made elsewhere in the flow.

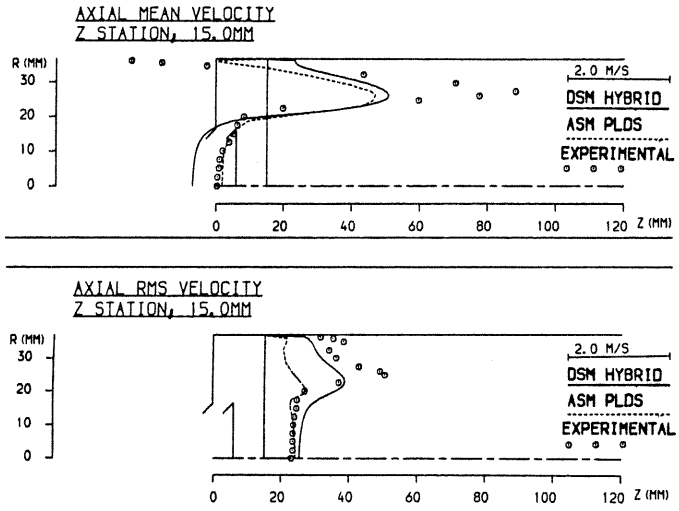

Fig. 8: Effects of corrected position of boundary conditions

Grid refinement. To test the levels of truncation errors contained within these results, a further run was made using the DSM, with the shifted inlet conditions, on a 109x73 line grid.

Figure 9 illustrates once again that the truncation errors are still large. Compared with Fig. 8, the mean axial velocity profile has changed appreciably. The jet is much thinner, resulting in a higher peak velocity, smaller backflow in the valve region, and a larger recirculation zone in the wall/head corner. However it must be noted that these mean flow results are still much inferior to the k-ϵ fine grid results, obtained using the QUICK scheme, as shown in Fig. 4. Note also that the ASM results shown are for the coarser grid.

The turbulence intensity predictions, however, are far superior, using the DSM. The two peaks in the near wall/jet profile are now close to being matched, being approximately 20% under-predicted. The major error now appears to lie in the region behind the valve, where the intensities are over-predicted by some 50%.

So far, only predictions of axial velocity profiles at the further measuring station have been presented. Figs. 10-12 show results, for the fine grid DSM calculations, of the radial profiles there, and at the other measuring location. The mean flow profiles at the valve face plane are exceptionally well predicted, even capturing the distinct kink in the axial velocity profile halfway from the valve edge to the wall. Predicted well too are the turbulence intensity profiles here. The three distinct peaks in each of the profiles is faithfully reproduced by the calculations. At the 15mm location, the radial profiles are reasonably predicted, particularly that of the turbulence intensity.

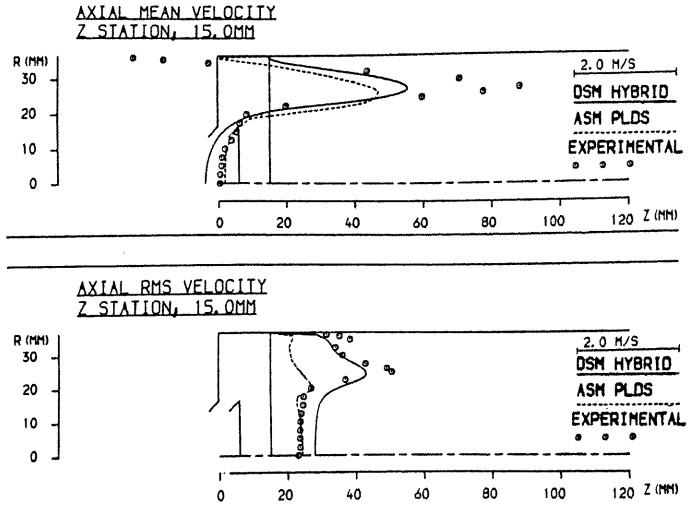

Fig. 9: Fine grid DSM results, axial profiles at 15 mm

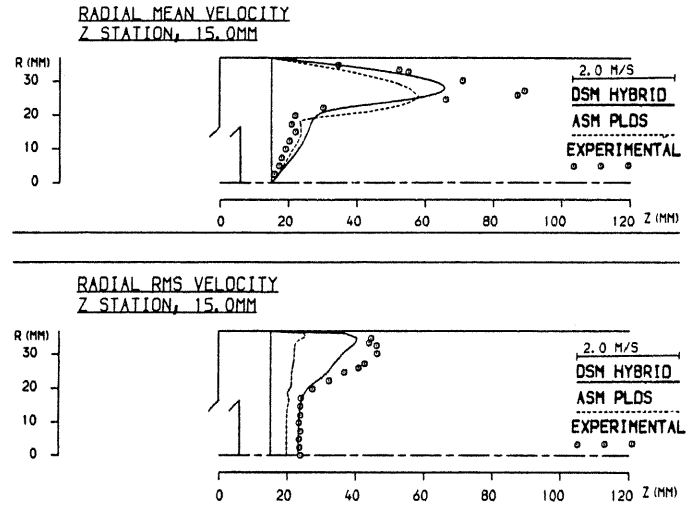

Fig. 10: Fine grid DSM results, radial profiles at 15 mm

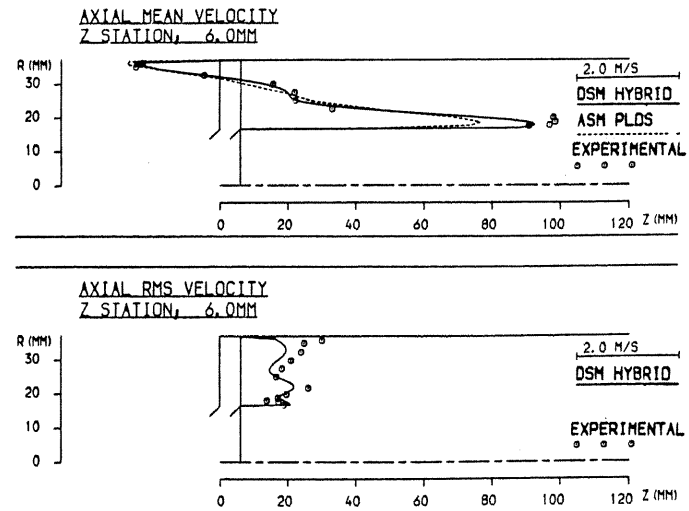

Fig. 11: Fine grid DSM results, axial profiles at 6 mm

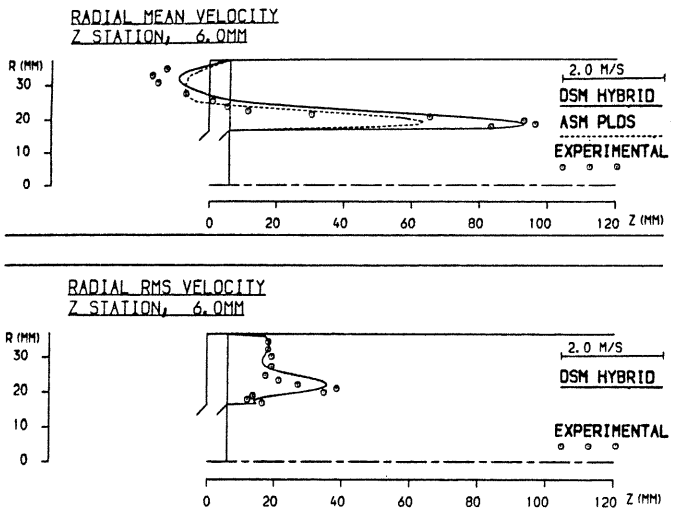

Fig. 12: Fine grid DSM results, radial profiles at 6 mm

CONCLUSIONS

It is clear from the results presented here that two or three dimensional in-cylinder flow calculations based on coarse grids, eddy-viscosity turbulence models and highly diffusive numerical schemes cannot hope to capture the fine details of the flow during intake. In particular the mean flow jet will be highly overpredicted in width and underpredicted in strength, and the turbulence intensities will be greatly under-predicted.

The main conclusions drawn from the results for this very simple geometry are that:

(i) to obtain accurate mean flow predictions the QUICK discretization scheme must be used, at least for the mean flow velocity components,
(ii) to obtain accurate turbulence intensity predictions a differential stress model of turbulence must be employed,
(iii) significant grid spacing truncation errors are still present in the calculations even when relatively fine grids (compared with most in-cylinder flow calculations) are used.

The QUICK scheme exhibits less grid truncation effects than do the diffusive HYBRID or PLDS schemes. It is to be hoped therefore that a combination of a differential stress model of turbulence with the QUICK scheme will allow more accurate solutions to be obtained on a coarser grid than found necessary here.

REFERENCES

1. Vafidis, C. and Whitelaw, J.H., "Steady and pulsating air flow through a stationary intake valve of a reciprocating engine", Imperial College, Mech. Eng. Dept. report, FS/84/04, 1984.
2. Launder, B.E. and Spalding, D.B., "The numerical computation of turbulent flows", Comput. Methods Appl. Mech. Eng., Vol. 3, pp. 269-289, 1974.
3. Rodi, W., ZAMM, Vol. 56, p. 219, 1975.
4. Launder, B.E., "Second moment closure and its use in modelling turbulent industrial flows", Int. J. Num. Methods in Fluids, Vol. 9, pp. 963-985, 1989.
5. Daly, B.J. and Harlow, F.H., "Transport equations in turbulence", Physics of Fluids, Vol. 13, pp. 2634-2649, 1970.
6. Rotta, J.C., Z. Phys., Vol. 129, p. 547, 1951.
7. Naot, D., Shavit, A. and Wolfshtein, M., Israel J. Technology, Vol. 8, p. 259, 1970.
8. Launder, B.E., Reynolds, W.C. and Rodi, W., Turbulence Models and Their Application, Eyrolles, Paris, 1984.
9. Fu, S., Huang, P.G., Launder, B.E. and Leschziner, M.A., "A comparison of algebraic and differential second-moment closures for axisymmetric turbulent shear flows with and without swirl", Trans. ASME, J. Fluids Eng., Vol. 110, pp. 216-221, 1988.
10. Patankar, S.V., Numerical Heat Transfer and Fluid Flow, Hemisphere, 1980.
11. Leonard, B.P., "A stable and accurate convective modelling procedure based on quadratic upstream interpolation", Comp. Methods in Appl. Mech. and Eng., Vol. 19, pp. 59-98, 1979.
12. Spalding, D.B., "A novel finite difference formulation for differential expressions involving both first and second derivatives", Int. J. for Num. Methods in Eng., Vol. 4, pp. 551-559, 1972.
13. Hanjalic, K. and Launder, B.E., "Sensitising the dissipation equation to irrotational strain", J. Fluids Engrg., Vol. 102, No.1, pp. 34-40, 1980.
14. Gosman, A.D., Johns, R.J.R. and Watkins, A.P., "Assessment of a prediction method for in-cylinder processes in reciprocating engines", Combustion Modelling in Reciprocating Engines, (Mattavi, J.N. and Amann, C.A. eds.), Plenum, 1980.
15. El-Tahry, S.H., "A comparison of three turbulence models in engine-like geometries", Int. Symp. on Diagnostics and Modelling of Combustion in Reciprocating Engines, Tokyo, 1985.